

## Supplementary Information

### **Synergistic enhancement of triethylamine sensing performances via oxygen vacancy-rich Co-doped MnO<sub>2</sub>@MnCo<sub>2</sub>O<sub>4.5</sub> nanorods/nanosheets**

Xiaobing Hu <sup>a</sup>, Hao Chen <sup>a</sup>, Kaibin Zhang <sup>a</sup>, Dongxia Tian <sup>a</sup>, Yi Cao <sup>a, c</sup>, Zhigang Zhu <sup>b</sup>,

\*

<sup>a</sup> Hubei Key Laboratory of Photoelectric Materials and Devices, School of Materials  
Science and Engineering, Hubei Normal University, Huangshi 435002, China

<sup>b</sup> School of Health Science and Engineering, University of Shanghai for Science and  
Technology, Shanghai 200093, China

<sup>c</sup> National Laboratory of Solid State Microstructures, Nanjing university, Nanjing  
210093, China

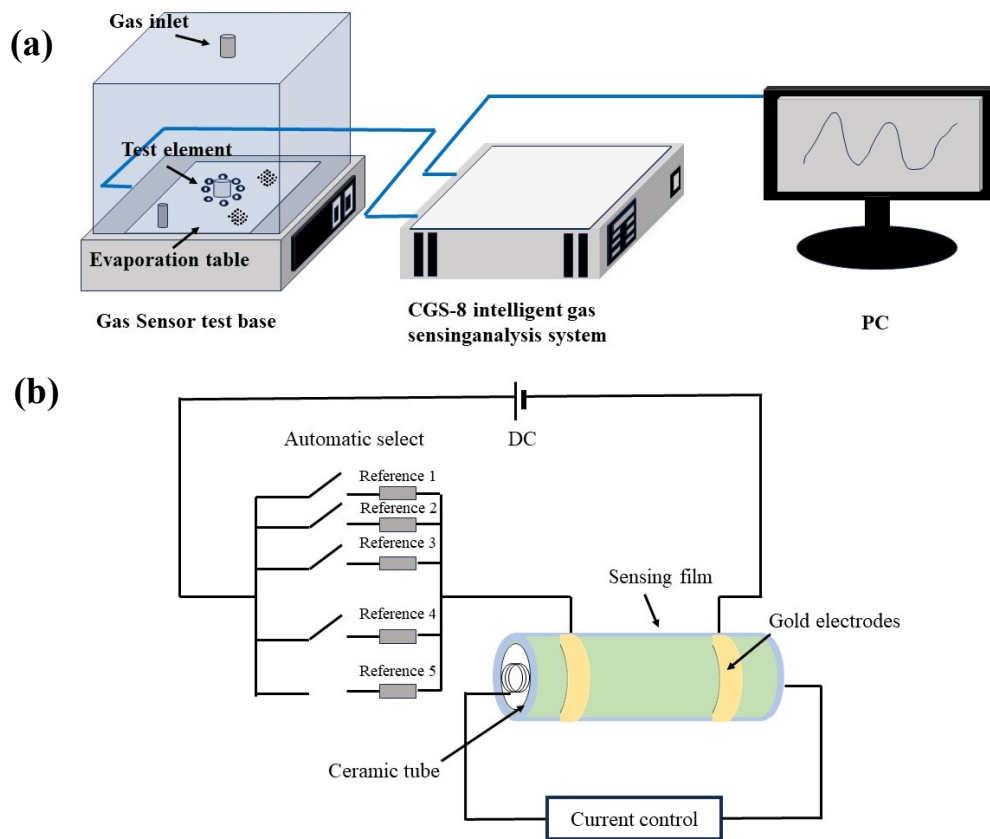


Fig. S1 (a) Schematic diagram of experimental device. (b) Schematic diagram of measuring resistance by DC voltage division method.

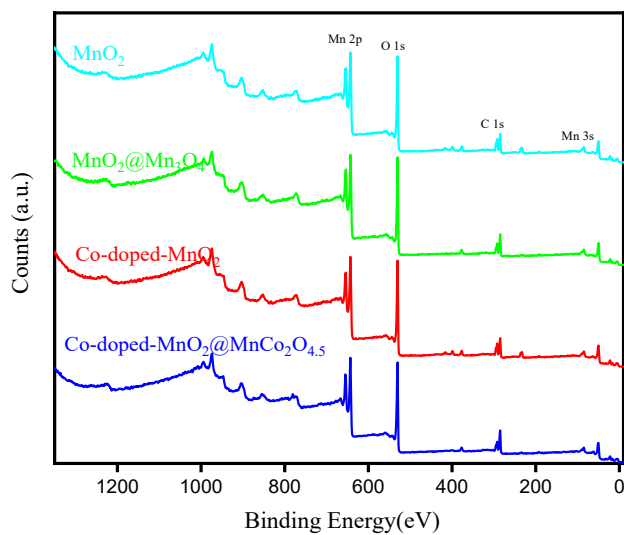


Fig. S2 XPS spectrum of the MnO<sub>2</sub>, MnO<sub>2</sub>@Mn<sub>3</sub>O<sub>4</sub>, Co-doped-MnO<sub>2</sub>, and Co-doped-MnO<sub>2</sub>@MnCo<sub>2</sub>O<sub>4.5</sub>.

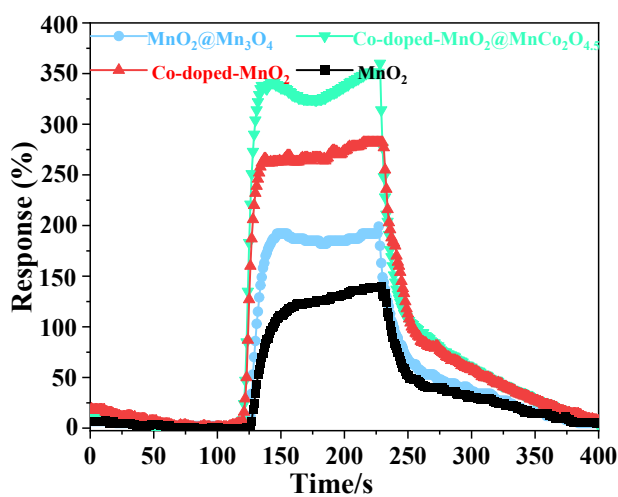


Fig. S3 Response and recovery curves of the sensors based on MnO<sub>2</sub>, MnO<sub>2</sub>@Mn<sub>3</sub>O<sub>4</sub>, Co-doped-MnO<sub>2</sub>, and Co-doped-MnO<sub>2</sub>@MnCo<sub>2</sub>O<sub>4.5</sub>.

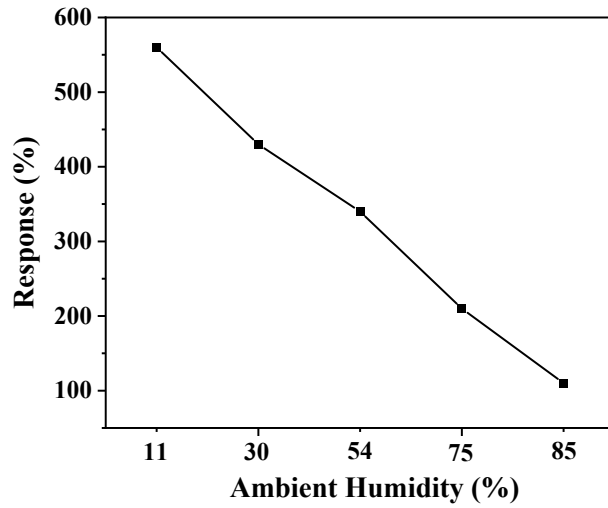


Fig. S4 Response of the Co-doped-MnO<sub>2</sub>@MnCo<sub>2</sub>O<sub>4.5</sub> to different relative humidity water vapor.

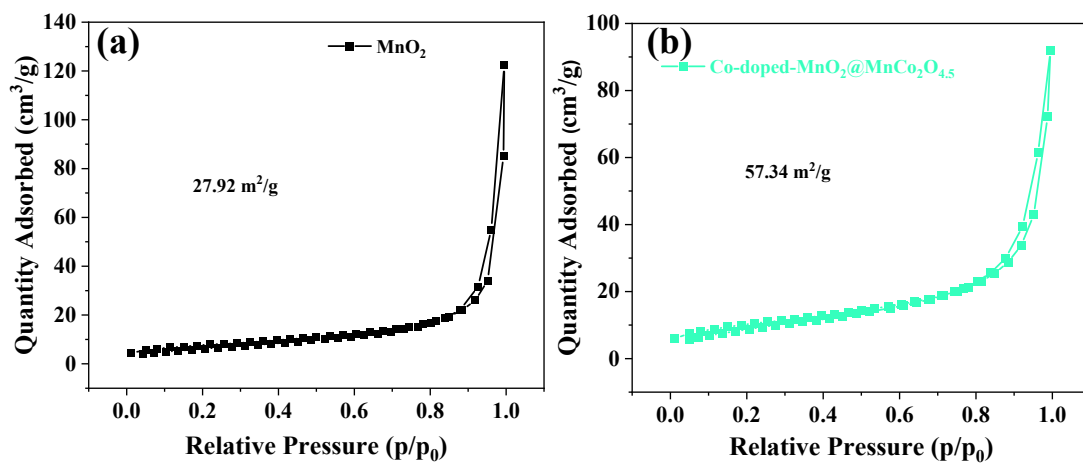


Fig. S6 Typical N<sub>2</sub> adsorption-desorption isotherms of different specimens: (a) MnO<sub>2</sub>, (b) Co-doped-MnO<sub>2</sub>@MnCo<sub>2</sub>O<sub>4.5</sub>.

